

Sol-Gel Synthesis of Zinc Oxide (ZnO) Nanoparticles: Study of Structural and Optical Properties

S. Jurablu, M. Farahmandjou*, and T. P. Firoozabadi

Department of Physics, Faculty of Science, Islamis Azad University, Varamin, Islamic Republic of Iran

Received: 18 February 2015 / Revised: 31 May 2015 / Accepted: 17 August 2015

Abstract

Zinc oxide (ZnO) nanopowders were synthesized by the sol-gel method from an ethanol solution of zinc sulfate heptahydrate in the presence of diethylene glycol surfactant. Detailed structural and microstructural investigations were carried out using x-ray diffraction (XRD), high-resolution transmission electron microscopy (HRTEM), field emission scanning electron microscopy (FE-SEM), Fourier transform infrared spectroscopy (FTIR) and UV-Vis spectrophotometer. XRD pattern showed that the zinc oxide nanoparticles exhibited hexagonal wurtzite structure. The average particle size of ZnO was achieved around 28 nm as estimated by XRD technique and direct HRTEM observation. The surface morphological studies from SEM and TEM depicted spherical particles with formation of clusters. The sharp peaks in FTIR spectrum determined the purity of ZnO nanoparticles and absorbance peak of UV-Vis spectrum showed the wide bandgap energy of 3.49 eV.

Keywords: ZnO nanoparticles; Sol-gel method; Crystal structure; Optical properties.

Introduction

Nanocrystalline materials have attracted a wide attention due to their unique properties and immense potential application in nano device fabrication. Zinc oxides of particle size in nanometer range have been paid more attention for their unique properties. They are widely used for solar energy conversion, non-linear optics, catalysis, varistors, pigments, gas sensors, cosmetics etc.[1-9]. Zinc oxide (ZnO) is an unexpensive, n-type semiconductor with a wide band gap having optical transparency in the visible range. It crystallizes in a hexagonal wurtzite structure (zincite) with lattice parameters as $c = 5.205 \text{ \AA}$, $a = 3.249 \text{ \AA}$. The n-type semiconductor behavior is due to the ionization of excess zinc atoms in interstitial positions and the

oxygen vacancies [10]. Surface defects play an important role in the photocatalytic activities of metal oxides as they increase the number of the active sites [11,12]. The structure of ZnO can be described as a number of alternating planes composed of tetrahedrally coordinated O^{2-} and Zn^{2+} stacked alternately along the c-axis, as shown in Figure 1. Various techniques for the preparation of ZnO nanopowders have been applied: sol-gel method [13-16], co-precipitation method [15,17] etc. Among the different methods, the sol-gel approach appears to be one of the most promising methods to prepare ZnO nanoparticles. Some of the most important advantages of the sol-gel method are: easiness of the synthesis, low temperature of decomposition and control on the chemical composition. These advantages make the sol-gel technique a very attractive preparation

* Corresponding author: Tel: +982122340298; Fax: +982122482091; Email: farahmandjou@iauvaramin.ac.ir

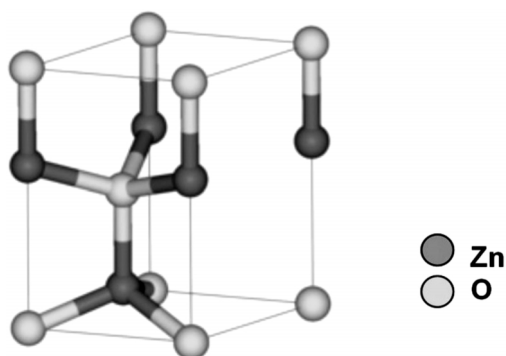


Figure 1. The wurtzite structure model of ZnO.

method, especially in the case of photocatalytically active ZnO powders [15]. In this work, a simple sol gel method was used to prepare ZnO nanoparticles. The aim of this study was to synthesize zinc oxide of low dimension and investigation of morphological properties and surfactant effect on the particle size. This method has novel features which are of considerable interest due to its low cost, easy preparation and industrial viability. Synthesis of ZnO nanoparticles by sol gel technique is reported by $\text{ZnSO}_4 \cdot 7\text{H}_2\text{O}$ precursor and calcined at 500°C . The structural and optical properties of ZnO have been studied by XRD, HRTEM, SEM, FTIR and UV-visible analyses.

Materials and Methods

ZnO nanoparticles were synthesized by a new sol gel approach according to the following manner. The 0.015 mol $\text{ZnSO}_4 \cdot 7\text{H}_2\text{O}$ (Merck) and 1.2 g diethylene glycol

(Merck) were added to mixed solution of 10mL ethanol (99.7% Merck) and 300 mL distilled water. The mixed solution stirred with a magnetic stirrer at 85°C for 2 hours to obtain the gel. The obtained gel was dried at 220°C for 1 hour then ground into a fine particle. The temperature of the dried precursor powder was increased at the rate of $1^\circ\text{C}/\text{min}$ to attain the required temperature and then allowed the sample to stay at 500°C for 3 hours to obtain the final product (i.e., ZnO nanoparticles). The specification of the size, structure and optical properties of the as-synthesis and annealed ZnO nanoparticles were carried out. X-ray diffractometer (XRD) was used to identify the crystalline phase and to estimate the crystalline size. The XRD pattern were recorded with 2θ in the range of $4\text{--}85^\circ$ with type X-Pert Pro MPD, $\text{Cu-K}\alpha$; $\lambda = 1.54 \text{ \AA}$. The morphology was characterized by field emission scanning electron microscopy (SEM) with type KYKY-EM3200, 25 kV and transmission electron microscopy (TEM) with type Zeiss EM-900, 80 kV. The optical properties of absorption were measured by ultraviolet-visible spectrophotometer (UV-Vis) with optima SP-300 plus, and Fourier transform infrared spectroscopy (FTIR) with WQF 510. All the measurements were carried out at room temperature.

Results

X-ray diffraction (XRD) at 40Kv was used to identify crystalline phases and to estimate the crystalline sizes. Figure 2(a) shows the XRD morphology of as-prepared ZnO nanoparticles and Figure 2(b) shows annealed sample at 500°C for 3 hours. In our case all

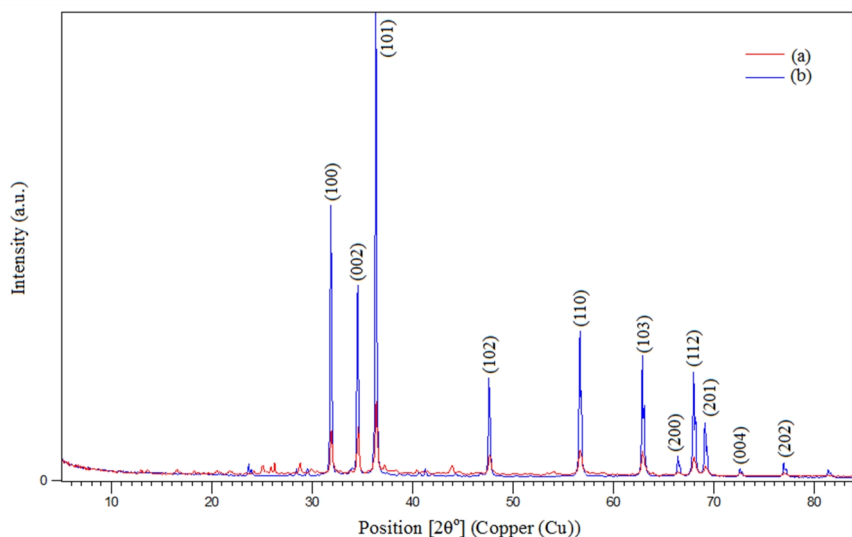


Figure 2. XRD pattern of ZnO nanoparticles: (a) as-synthesized and (b) annealed samples at 500°C for 3 hours

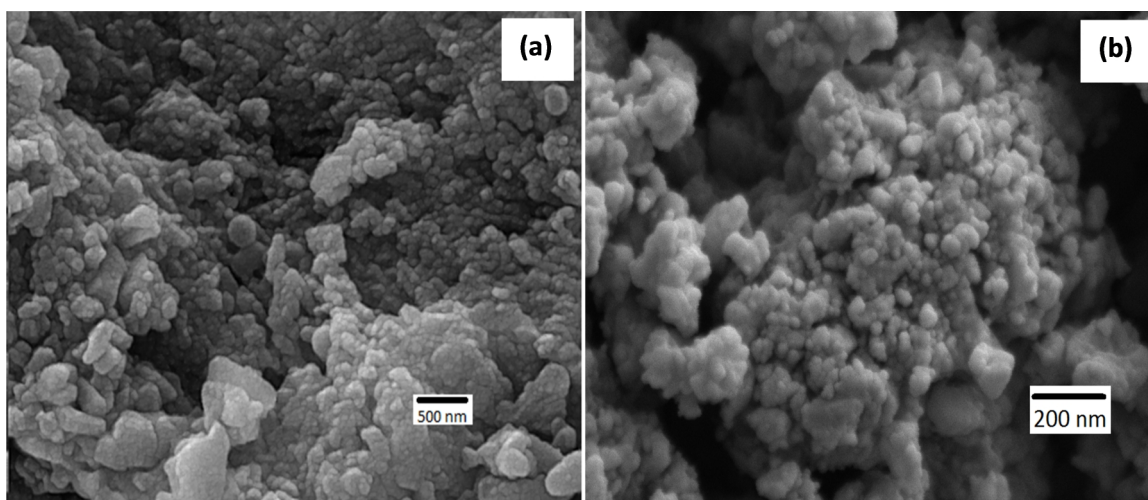


Figure 3. FE-SEM images of the ZnO nanoparticles: (a) as-prepared (b) annealed at 500°C for 3 h

the diffraction peaks at angles (2θ) of 31.36°, 34.03°, 35.8°, 47.16°, 56.26°, 62.54°, 67.64°, 68.79°, 69.45°, 72.82° and 77.33° correspond to the reflection from (100), (002), (101), (102), (110), (103), (200), (112), (201), (004) and (202) crystal planes of the hexagonal wurtzite zinc oxide structure. The mean size of the ordered ZnO nanoparticles has been estimated from full width at half maximum (FWHM) and Debye-Scherrer formula according to equation the following:

$$D = \frac{0.89\lambda}{B \cos \theta} \quad (1)$$

where, 0.89 is the shape factor, λ is the x-ray wavelength, B is the line broadening at half the maximum intensity (FWHM) in radians, and θ is the Bragg angle. The mean size of as-prepared ZnO nanoparticles was around 25 nm from this Debye-Scherrer equation.

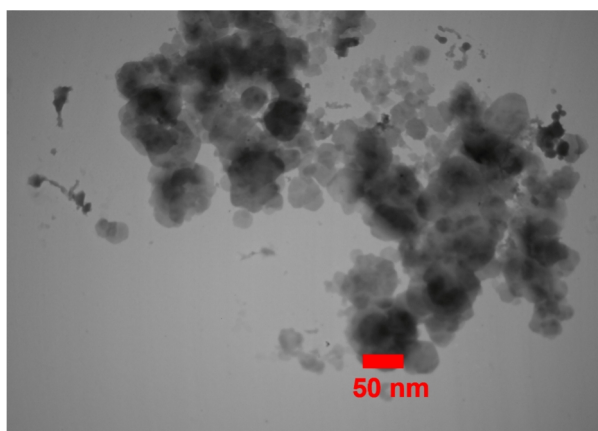


Figure 4. TEM images of the as-prepared ZnO nanoparticle

FE-SEM analysis was used for the morphological study of nanoparticles of ZnO. These analyses show that high homogeneity emerged in the samples surface by increasing annealing temperature. With increasing temperature the morphology of the particles changes to the spherical shape and nanopowders were less agglomerate. Figure 3(a) shows the SEM image of the as-prepared ZnO nanoparticles prepared by sol-gel method. In this figure, the particles prepared with formation of clusters. Figure 3(b) shows the SEM image of the annealed ZnO nanoparticles at 500°C for 3 hours. The ZnO nanoparticles formed were less agglomerated. The crystallite size of annealed nanocrystals is in the range of 20-80 nm in diameter.

TEM analysis was carried out to confirm the actual size of the particles, their growth pattern and the distribution of the crystallites. Figure 4 shows the as-synthesized TEM image of ZnO nanoparticles prepared by sol gel route with an average diameter about 28 nm.

Figure 5 shows the FT-IR spectra of the ZnO powders, which were acquired in the range of 4000 to 400 cm^{-1} . All of the spectra exhibit a strong absorption peak at 3508 cm^{-1} for stretching vibration of non-chemical bond association OH groups and at 1637 cm^{-1} for H-O-H bending vibrations. The peaks at 2390 cm^{-1} are attributed to the presence of carbon dioxide. The absorption picks around 1392 cm^{-1} is assigned to the bending vibration of C-H stretching. The peaks at 514 to 442 cm^{-1} are for Zn-O. The above results are in accordance with the XRD results.

UV-Vis absorption spectra of as-prepared and annealed TiO₂ nanoparticles are shown in Figure 6. For as-synthesized TiO₂ nanoparticles, the strong absorption band at low wavelength near 355 nm ($E_g=3.49$) for anatase in Figure 6(a) and for annealed TiO₂

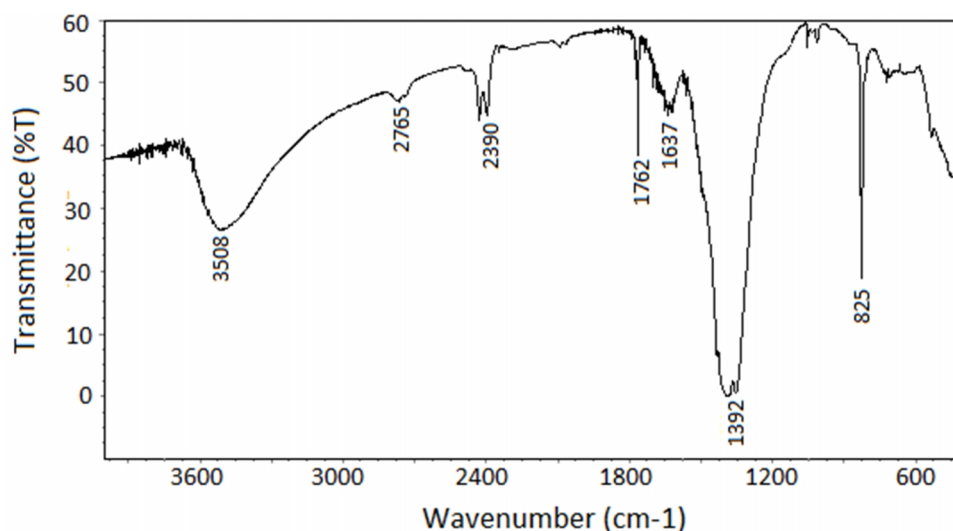


Figure 5. The FTIR pattern of the zinc oxide nanoparticles

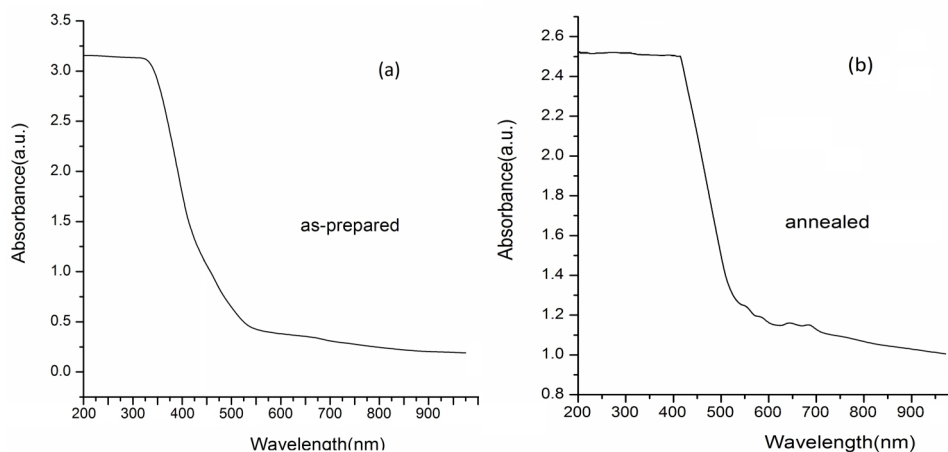


Figure 6. UV-Vis absorption spectra of TiO_2 nanoparticles: (a) as-prepared and (b) annealed samples

nanoparticles the strong absorption band at low wavelength near 410 nm ($E_g=3.02$) for rutile phase in Figure 6(b) indicate the presence of phase transition of anatase to rutile for TiO_2 nanoparticles under heat treatment at 500°C [18]. The absorption edge extends to longer wavelengths for TiO_2 nanoparticles, and absorption tail in the visible-light region over 350–500 nm and strong absorption band in the UV-light region is clearly observed. It indicates the absorption positions depend on the morphologies and sizes of ZnO. The UV absorption ability of ZnO is related with band gap energy. The UV-absorption edge provides a reliable estimate of the band gap of any system.

Discussion

In summary, we have analyzed the composition of ZnO particles synthesized by a new sol gel method using $\text{ZnSO}_4 \cdot 7\text{H}_2\text{O}$ and diethylene glycol as surfactant. The XRD and TEM results show that these nanoparticles are hexagonal wurtzite in phase ZnO with a mean grain size of about 28 nm. From SEM images, it is clear that with increasing temperature the morphology of the particles changes to the spherical shape and nanopowders were less agglomerate. TEM image exhibits that the as-synthesized ZnO nanoparticles prepared by sol gel route with an average diameter about 28 nm. From the FTIR data, it is shown the presence of Zn-O stretching mode of ZnO. The absorbance peak of UV-Vis spectrum showed the wide

bandgap energy of 3.49 eV for as-prepared samples.

References

1. Sakohapa S., Tickazen L. and Anderson M. Luminescence properties of thin zinc oxide membranes prepared by the sol-gel technique: change in visible luminescence during firing. *J. phys. Chem.* **96**: 11086-11091 (1992).
2. Harada K., Asakura K., Ueki Y. and Toshina N. Structure of polymer-protected palladium-platinum bimetallic clusters at the oxidized state: extended x-ray absorption fine structure analysis. *J. phys. Chem.* **96**: 9730-9738 (1992).
3. Lee J., Hwang J., Mashek T., Mason T., Miller A. and Siegel R. Impedance spectroscopy of grain boundaries in nanophase ZnO. *J. Mater. Res.* **10**: 2295-2300 (1995).
4. Hara K., Horiguchi T., Kinoshita T., Sayama K., Sugihara H. and Arakawa H. Highly efficient photon-to-electron conversion with mercurochrome-sensitized nanoporous oxide semiconductor solar cells. *Sol. Energy mater Sol. Cells.* **64**: 115-134 (2000).
5. Gao P. and Wang Z. Nanoarchitecture of Semiconducting and Piezoelectric ZnO. *J. Appl. phys.* **97**: 044304-044311 (2005).
6. Ko S., Kim Y., Lee S., Choi S. and Kim S. Micromachined piezoelectric membrane acoustic device. *Sensors and Actuators A, Physical.* **103**: 130-134 (2003).
7. Sberveglieri G., Gropelli S., Nelli P., Tintinelli A. and Giunta G. A novel method for the preparation of NH₃ sensors based on ZnO-In thin films. *Sens. Actual B.* **25**: 588-590 (1995).
8. Shishiyance S., Shishiyance T. and Lupan O. Sensing characteristics of tin-doped ZnO thin films as NO₂ gas sensor. *Sens. Actual B.* **107**: 379-386 (2005).
9. Han J. and Kim D. Fabrication of dense ZnO-varistors by atmosphere sintering. *J. European Ceramic. Soc.* **18**: 765-770 (1998).
10. Bahsi Z. and Oral A. Effects of Mn and Cu Doping on the Microstructures and Optical Properties of Sol-gel Derived ZnO Thin Films. *Opt. Mater.* **29**: 672-678 (2007).
11. Rekha K., Nirmala M. Nair M. and Anukaliani A. Structural, optical, photocatalytic and antibacterial activity of zinc oxide and manganese doped zinc oxide nanoparticles. *Physica B: Condensed Matter.* **405**: 3180-3185 (2010).
12. Ullah R. and Dutta j. Photocatalytic degradation of organic dyes with manganese-doped ZnO nanoparticles. *J. Hazard. Mater.* **156**: 194-200 (2008).
13. Fu M., Li Y., Wu S., Lu P., Liu J. and Dong F. Sol-gel preparation and enhanced photocatalytic performance of Cu-doped ZnO nanoparticles. *Appl. Surf. Sci.* **258**: 1587-1591 (2011).
14. Xu C., Cao L., Su G., Liu W., Liu H., Yu Y. and Qu X. Preparation of ZnO/Cu₂O compound photocatalyst and application in treating organic dyes. *J. Hazard. Mater.* **176**: 807-813 (2010).
15. Liu Z., Deng J., Deng J. and Li F. Fabrication and photocatalysis of CuO/ZnO nano-composites via a new method. *Mater. Sci. Eng. B.* **150**: 99-104 (2008).
16. Fernandes D., Silva R., Hechenleitner A., Radovanovic E., Melo M. and Pineda E. Synthesis and characterization of ZnO, CuO and a mixed Zn and Cu oxide. *Mater. Chem. Phys.* **115**: 110-115 (2009).
17. Muthukumar S. and Gopalakrishnan R. Structural, FTIR and photoluminescence studies of Cu doped ZnO nanopowders by co-precipitation method, *Opt. Mater.* **34**: 1946-1953 (2012).
18. Cao Y., Zhao Z., Yi J., Ma C., Zhou D., Wang R., Li C. and Qiu J. Luminescence properties of Sm³⁺-doped TiO₂ nanoparticles: Synthesis, characterization, and mechanism, *J. Alloys Compounds.* **554**: 12-20 (2013).